inorganics

MDPI

Article

Reduction of Triple Bond in $[B_{12}H_{11}NCR]^-$ Anions by Lithium Aluminum Hydride: A Novel Approach to the Synthesis of N-Monoalkylammonio-Substituted *closo*-Dodecaborates

Alexey V. Nelyubin [1], Nikolay K. Neumolotov [1], Nikita A. Selivanov [1], Alexander Yu. Bykov [1], Ilya N. Klyukin [1], Alexander S. Novikov [2,3], Alexey S. Kubasov [1], Andrey P. Zhdanov [1,*], Konstantin Yu. Zhizhin [1,*] and Nikolay T. Kuznetsov [1]

[1] Kurnakov Institute of General and Inorganic Chemistry, Russian Academy of Sciences, Leninskii Pr. 31, 119991 Moscow, Russia; nelyubin.av@yandex.ru (A.V.N.); neumolotovn@gmail.com (N.K.N.); goovee@yandex.ru (N.A.S.); bykov@igic.ras.ru (A.Y.B.); klukinil@igic.ras.ru (I.N.K.); fobosax@mail.ru (A.S.K.); boron@igic.ras.ru (N.T.K.)

[2] Institute of Chemistry, Saint Petersburg State University, Universitetskaya Nab. 7-9, 199034 Saint Petersburg, Russia; a.s.novikov@spbu.ru

[3] Research Institute of Chemistry, Peoples' Friendship University of Russia (RUDN University), Miklukho-Maklaya St. 6, 117198 Moscow, Russia

* Correspondence: zhdanov@igic.ras.ru (A.P.Z.); zhizhin@igic.ras.ru (K.Y.Z.)

Abstract: By reacting nitrilium derivative of the *closo*-dodecaborate anion, $Bu_4N[B_{12}H_{11}N{\equiv}CR]$ (where R = Me, Et, nPr, iPr, p-tolyl), with lithium aluminum hydride ($LiAlH_4$), N-alkylammonium derivatives of the *closo*-dodecaborate anion, and $Bu_4N[B_{12}H_{11}NH_2CH_2R]$, were obtained. The reduction reaction procedure was optimized, achieving yields close to quantitative (90–95%). The structure of the compound $Bu_4N[B_{12}H_{11}NH_2CH_2CH_3]$ was determined using X-ray structural analysis. It was found that substituting lithium aluminum hydride ($LiAlH_4$) with sodium borohydride ($NaBH_4$) leads to the same products but only upon heating, while the reaction with $LiAlH_4$ proceeds at room temperature.

Keywords: nitrilium derivative; *closo*-dodecaborate anion; reduction

check for updates

Citation: Nelyubin, A.V.; Neumolotov, N.K.; Selivanov, N.A.; Bykov, A.Y.; Klyukin, I.N.; Novikov, A.S.; Kubasov, A.S.; Zhdanov, A.P.; Zhizhin, K.Y.; Kuznetsov, N.T. Reduction of Triple Bond in $[B_{12}H_{11}NCR]^-$ Anions by Lithium Aluminum Hydride: A Novel Approach to the Synthesis of N-Monoalkylammonio-Substituted *closo*-Dodecaborates. *Inorganics* **2024**, *12*, 2. https://doi.org/10.3390/inorganics12010002

Academic Editor: Michael A. Beckett

Received: 7 November 2023
Revised: 12 December 2023
Accepted: 16 December 2023
Published: 20 December 2023

Copyright: © 2023 by the authors. Licensee MDPI, Basel, Switzerland. This article is an open access article distributed under the terms and conditions of the Creative Commons Attribution (CC BY) license (https://creativecommons.org/licenses/by/4.0/).

1. Introduction

Higher polyhedral boranes $[B_nH_n]^{2-}$ (n = 10, 12) are the subjects of numerous studies. Traditionally, boron cluster anions are used as agents for boron neutron capture therapy (BNCT) [1–5], high-energy materials, non-coordinating anions, and ligands [6–12]. In recent years, this class of compounds has been utilized as optical [13–17] and magnetic [18–21] materials, chemical reaction catalysts [22–25], and materials for photovoltaics [26–28].

The *closo*-dodecaborate dianion $[B_{12}H_{12}]^{2-}$ is a spatially aromatic system with delocalized electrons, which accounts for the high thermal and kinetic stability of its derivatives and their tendency to undergo substitution reactions of the *exo*-polyhedral hydrogen atom [29]. Due to the high symmetry of the *closo*-dodecaborate anion $[B_{12}H_{12}]^{2-}$ (symmetry group I_h), the anion lacks a distinct reaction center. Consequently, obtaining monosubstituted derivatives of the *closo*-dodecaborate anion is often complicated by the formation of poly-substituted products.

Hydrogen atom substitution reactions can proceed via radical mechanisms. Such processes include reactions of exhaustive halogenation of the free anion $[B_{12}H_{12}]^{2-}$ and its substituted derivatives [30–33], as well as the formation of *closo*mer anions $[B_{12}(OH)_{12}]^{2-}$ and $[B_{12}(OH)_{11}NH_3]^-$ [34,35]. Electrophilic processes are used to obtain carbonyl derivatives [36], halogen-*closo*-dodecaborates with low degrees of substitution [37] and alkyl and aryl derivatives [38]. The reaction of $[B_{12}H_{12}]^{2-}$ anion with hydroxylamine-O-sulfonic acid

proceeds through an electrophilic mechanism [39]. This process can be characterized as stepwise; it strongly depends on the reaction conditions and the ratio of reagents and often leads to the formation of a mixture of mono- and di-substituted products in the form of 1,2-, 1,7-, and 1,12-isomers [32]. The latter can be separated by chromatographic methods or fractional crystallization. The most selective process for the preparation of mono-substituted *closo*-dodecaborates is nucleophilic substitution proceeding via the EINS mechanism [40]. This approach allows the preparation of derivatives based on cyclic and simple esters, organic acids and amides based on them, and thioureas [29,41]. Methods based on the modification of substituents introduced into the cluster are actively used for the directed synthesis of functionalized *closo*-dodecaborates. Such processes include alkylation and acylation reactions of hydroxy groups and thiols [42–47], opening of oxonium substituents [41,48,49], *ipso*-substitution of halogen atoms [50,51], and iodonium substituents [52,53].

Previously, alkylammonium derivatives of the *closo*-dodecaborate anion were obtained through the reduction of the reaction products of ammonium derivatives with aldehydes using sodium borohydride ($NaBH_4$) [54]. Using this method, derivatives with the composition $[B_{12}H_{11}NH_2CH_2R]$ were successfully obtained but only with aryl substituents (R = 2-C_6H_4-OMe, 3,4-$C_6H_3O_2CH_2$, 4-$C_6H_4NHCOMe$, 4-C_6H_4CN). It is noteworthy that the work lacks data on the synthesis of derivatives with aliphatic substituents.

Another method for obtaining alkylammonium derivatives is the direct alkylation of $[B_{12}H_{11}NH_3]^-$, and the products depend on the nature of the alkyl group [55,56]. For instance, when R = CH_3 or C_2H_5, alkylation leads to the formation of trialkyl-substituted derivatives $[B_{12}H_{11}NR_3]^-$. Increasing the length of the substituent chain results in the formation of disubstituted derivatives $[B_{12}H_{11}NHR_2]^-$ due to steric factors. The synthesis of monoalkyl-substituted derivatives is complicated because, even with a 1:1 ratio, a mixture of mono- and poly-substituted products is formed. Therefore, the challenge of selectively obtaining monoalkyl-substituted derivatives of *closo*-dodecaborate anion with different substituent types remains unresolved.

Nitrilium derivatives of the *closo*-dodecaborate anion $[B_{12}H_{11}N{\equiv}CR]^-$ have great potential for modification due to the labile N≡C bond [57–59]. For a long time, it was believed that these derivatives could not be isolated in their non-hydrolyzed form [58]. However, a new synthesis method involving the use of absolute organic solvents allows the preparation of these compounds in pure form and for further modifications [60].

Previously in our laboratory, it was demonstrated that the reduction of nitrile derivatives of the *closo*-dodecaborate anion $[B_{10}H_9N{\equiv}CR]^-$ using $LiAlH_4$ in an anhydrous, aprotic solvent leads to the formation of alkylammonium derivatives with the composition $[B_{10}H_9NHCH_2R]^-$ (R = CH_3, C_2H_5, *n*-Pr, *t*-Bu, Ph, 1-Naph) [61]. In the present study, we applied this approach to obtain monoalkylammonium derivatives of the *closo*-dodecaborate anion $[B_{12}H_{11}NHCH_2R]^-$ with alkyl and aryl substituents.

2. Results

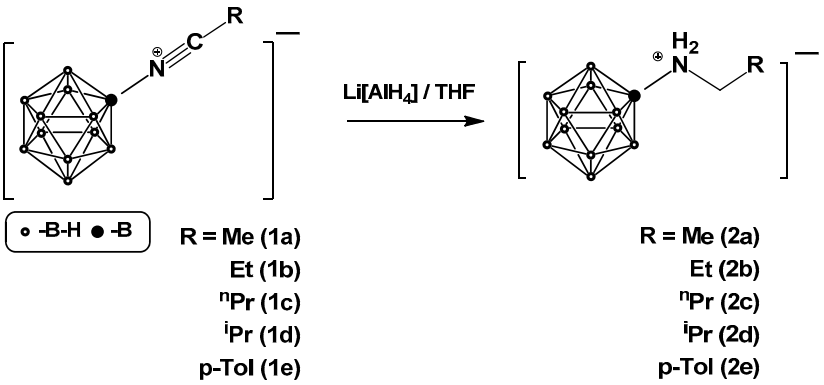
Lithium aluminum hydride (LAH) is widely used for the reduction of various functional groups, including carbonyl groups [62,63], nitriles [64–67], and others [68,69]. Nitriles containing the -CN functional group can be reduced by LAH to primary amines [70]. This process is of great importance because amines are significant building blocks in organic synthesis, including the development of pharmaceuticals, agrochemicals, and other specialized organic compounds. The reduction mechanism of LAH nitriles involves several key steps [71]. First, lithium aluminum hydride interacts with the nitrile group, leading to the formation of an imine and an aluminate complex. Next, the imine is reduced to the primary amine. An important feature of this reaction is its high stereospecificity and ability to form products in high yields.

The reduction of nitriles by LAH is a preferred method over other reducing agents such as sodium borohydride ($NaBH_4$) because of its higher reactivity and ability to reduce a wider range of functional groups [72]. In addition, LAH efficiently reduces nitriles under mild conditions, which minimizes the risk of degradation of sensitive functional groups

or formation of byproducts. In addition, the choice of solvent for reaction with LAH is crucial. Typically, ether solvents such as diethyl ether or tetrahydrofuran (THF) are used because they stabilize the alumohydride anion and prevent spontaneous decomposition of the reagent.

As previously demonstrated, the reduction of nitrile derivatives of the *closo*-decaborate anion $(Bu_4N)[B_{10}H_9N{\equiv}CR]$ with lithium aluminum hydride leads to the formation of monoalkylammonium derivatives with the substituent RCH_2^-. In the present study, a similar approach was used for the first time to obtain a series of monoalkylammonio-*closo*-dodecaborates with the composition $(Bu_4N)[B_{12}H_{11}NH_2CH_2R]$ (R = Me, Et, nPr, iPr, p-tolyl) from the corresponding nitrile derivatives $(Bu_4N)[B_{12}H_{11}N{\equiv}CR]$. The reaction proceeds selectively under mild conditions with near quantitative in situ yields (90–95%) and high isolated yields (79–90%).

The reaction was conducted in anhydrous tetrahydrofuran (THF) at room temperature with a 7-fold excess of $Li[AlH_4]$ (Scheme 1) within 2 h. A multiple excess of LAH is due to the reagent grade of the reagent (95%). Purification of the resulting product was not complicated and featured few steps. Firstly, 10 mL of 1N HCl was added to the solution until evaluation of gas ceased. After collecting, precipitate was washed with 20 mL of acetonitrile, and filtrate solution was concentrated. The last purification step was to remove any remaining byproducts by washing with 20 mL of diethyl ether. When the suspension of $Li[AlH_4]$ was added to the nitrile derivative solution, the mixture acquired a light-yellow color, which later faded. A similar change in color was observed when sodium borohydride ($Na[BH_4]$) was used. This phenomenon can be explained by the formation of a colored intermediate during the reaction. Also, in contrast to the *closo*-decaborate anion, the formation of degradation products of the boron cluster (and the formation of boronium adducts) is not observed in the reaction mixture due to the greater stability of the twelve-vertex polyhedron.



Scheme 1. Reaction of nitrilium derivatives with lithium aluminum hydride.

The reactions were monitored using ^{11}B NMR spectroscopy by taking an aliquot of reacting THF solution and quenching with 1N HCl until pH < 7. Purity of resulted individual compounds was determined via the HPLC method (40% of MeCN/60% of 0.2% CF_3COOH in H_2O). The spectra of nitrile derivatives $(Bu_4N)[B_{12}H_{11}N{\equiv}CR]$ differ from those of $(Bu_4N)_2[B_{12}H_{12}]$ by the presence of a small shoulder in the region close to the main peak (−15.1 ppm). Depending on the nature of the substituent, the signal from the substituted position (B1) can be well distinguished (e.g., a singlet at −12.0 ppm for $(Bu_4N)[B_{12}H_{11}N{\equiv}CC_2H_5]$) or completely merge with the signal from the unsubstituted positions (as in the case of $(Bu_4N)[B_{12}H_{11}N{\equiv}CC_6H_4CH_3]$). This difference in the nitrile derivatives from other derivatives of the *closo*-dodecaborate anion is related to the presence of a cone of magnetic anisotropy in the -N≡C-bond.

During the reduction of the triple bond, the shielding effect significantly weakens. For example, in the ^{11}B NMR spectrum of $(Bu_4N)[B_{12}H_{11}NH_2CH_2C_2H_5]$, three signals are clearly distinguishable: −5.5 ppm (B1, singlet), −16.8 ppm (B2-B11, doublet),

and −19.6 ppm (B12, singlet). The two hydrogen atoms attached to the nitrogen atom (-N**H$_2$**CH$_2$C$_2$H$_5$) are detected in the ^{1}H NMR spectrum as a broad signal at 4.87 ppm. The hydrogen atoms of the propyl group are observed as multiplets at 2.83 (C**H$_2$**CH$_2$CH$_3$), 1.58 (2H, CH$_2$C**H$_2$**CH$_3$), and a triplet at 0.88 ppm (CH$_2$CH$_2$C**H$_3$**). Additionally, characteristic signals from the Bu_4N^+ cation are present in the spectrum at 3.15, 1.61, 1.45, and 1.01 ppm.

The eleven hydrogen atoms from the B-H bonds of the cluster are in a broad range from 0 to 2.5 ppm. The carbon atoms of the propyl group are detected in the ^{13}C NMR spectrum. The signals at 50.6, 22.2, and 11.3 ppm correspond to the α, β, and γ carbon atoms, respectively.

The change in the *exo*-polyhedral substituent structure is also evident from the IR spectra data. Two characteristic types of absorption bands are observed in the spectra of $[B_{12}H_{11}NH_2CH_2R]^-$ products. The absorption band of the valence vibrations of the B-H bond is in the region of 2495–2490 cm^{-1}. Two absorption bands in the ranges 3290–3230 and 3206–3195 cm^{-1} correspond to the valence vibrations of the N-H bonds of the ammonium group. Also, the absorption bands of the C≡N bond in the region 2330–2300 cm^{-1} are absent in the spectra of the reduction products [60].

The compound **2a** crystallizes in a monoclinic crystal system (space group P2$_1$/n, Table 1). The crystallographically independent part of the elementary cell contains one cation Bu_4N^+ and one anion $[B_{12}H_{11}NH_2Et]^-$. The boron cluster is an icosahedron with slightly distorted geometry, which may be due to the presence of a charged *exo*-polyhedral substituent. The lengths of B-B bonds are in the range 1.760(5)–1.808(5) Å (Table 1). The B-N bond length in the anion is 1.587(4) Å (Figure 1), which is slightly more than in the unsubstituted ammonium derivatives [32,73], but corresponds well with the previously described anion $[B_{12}H_{11}NH_2iPr]^-$ [56]. Also, this parameter is comparable to the B-N bond length in the anion $[2\text{-}B_{10}H_9NH_2CH_2CH_3]^-$ (1.569 Å) [61] and borane adducts with primary amines (*n*-propylamine B-N bond 1.593 Å [74] and ethylenediamine 1.60 Å [75]). The N1-C1 bond length is 1.432(4) Å, which is slightly shorter than the analogous bond in the substituted N-ethylammonio *closo*-decaborate and borane adducts. The values of the B1-N1-C1 and N1-C1-C2 angles indicate a distorted tetrahedral environment of the N1 and C1 atoms. The ethylammonium substituent itself in the crystal has a geometry close to planar. Thus, the dihedral angle B1-N1-C1-C2 is 167.9(3)°. This geometry of the substituent is explained by the formation of rather strong intermolecular dihydrogen bonds. In solutions these interactions are probably leveled, which is consistent with the ^{1}H NMR data. Thus, no enantiomeric splitting of signals of methylene protons of NH$_2$-C**H$_2$** groups, which is characteristic of molecules with difficult rotation of the substituent around the N-C bond, is observed [76,77]. In addition, in IR spectra of solutions of the obtained compounds, there is no additional cleavage of B-H bond bands.

Table 1. Crystal data and structure refinement for **2a**.

Compound	**2a**
Empirical formula	$C_{18}H_{54}B_{12}N_2$
Formula weight	428.35
Temperature/K	150.00
Crystal system	monoclinic
Space group	P2$_1$/n
a/Å	10.292(12)
b/Å	12.938(10)
c/Å	21.49(3)
β/°	90.15(6)
	90
Volume/Å^3	2862(5)
Z	4
ρ_{calc}g/cm^3	0.994
μ/mm^{-1}	0.050
F(000)	944.0

Table 1. *Cont.*

Compound	2a
Radiation	MoKα (λ = 0.71073)
2Θ range for data collection/°	3.674 to 51.994
Reflections collected	11,524
Independent reflections	5562 [R_{int} = 0.0379, R_{sigma} = 0.0722]
Data/restraints/parameters	5562/7/295
Goodness of fit on F^2	1.057
Final R indexes [I >= 2σ (I)]	R_1 = 0.0783, wR_2 = 0.2136
Final R indexes [all data]	R_1 = 0.1340, wR_2 = 0.2438

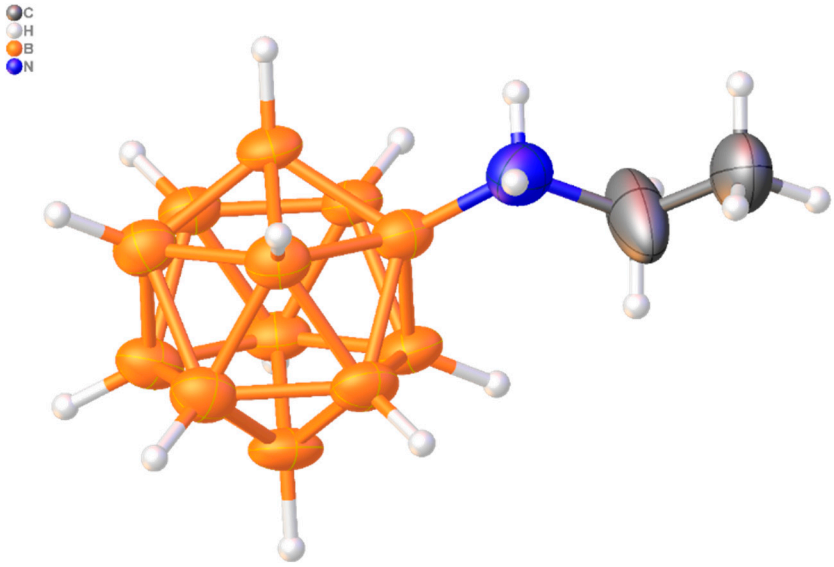


Figure 1. The structure of the anion $[B_{12}H_{11}NH_2Et]-$ according to X-ray structural analysis. Thermal ellipsoids are shown with a 50% probability. Selected bond lengths and angles in the structure of **2a**: lengths, Å: B1-N1 1.587(4); N1-C1 1.432(4); C1-C2 1.487(5); B-B 1.760(5)-1.808(5) (1.783 avg.); angles, °: B1-N1-C1 119.4(3); N1-C1-C2 116.4(3).

In the crystal, the anions $[B_{12}H_{11}NH_2Et]^-$ connected to each other via numerous non-covalent contacts. For the investigation of non-covalent contact, combined Hirshfeld surface analysis and the QTAIM approach were used (Figures 2b and S21). According to Hirshfeld analysis, the major contribution to the connection between anions is made by NH. . .HB contacts (Figure 2b, red spots on the Hirshfeld surface of the anion), which are shown on the fingerprint plots as two adjacent peaks with d_i and d_e alternately equal to 1.00 Å and 1.03 Å. The distances of NH. . .HB contacts lie in the range between 2.15 and 2.20 Å. According to QTAIM analysis, the values of electron density *p(r)* at bond critical points (bcp) related to NH. . .HB contacts are equal to 0.008 e $Å^{-3}$. The values of Laplacian of electron density $\nabla^2 p(r)$ lie in the range 0.024–0.025 e $Å^{-5}$. The values of total energy H_b are positive and equal to 0.001 h e^{-1}. It is interesting to compare present results with those previously obtained for the $[B_{12}H_{11}NH{=}C(CH_3)NH_2]^-$ anion [58]. For the $[B_{12}H_{11}NH{=}C(CH_3)NH_2]^-$ system, intramolecular NH. . .HB contacts were considered, whereas in the case of $[B_{12}H_{11}NH_2Et]^-$ analogous contacts are intermolecular. Based on data of QTAIM analysis, one can conclude that intramolecular NH. . .HB contacts are stronger compared to intermolecular ones. The NH. . .HB contacts' cluster anions are linked to each other by CH. . .HB contacts and form a column parallel to the a-axis, surrounded by tetrabutylammonium cations. One hundred percent of the anion's surface is accounted for by H. . .H contacts with tetrabutylammonium cations and adjacent anions. The distances of CH. . .HB contacts lie in the range between 2.42 and 2.56 Å. The values of electron density *p(r)* at bcp related to CH. . .HB contacts lie in the range 0.004–0.005 e $Å^{-3}$. The values of

Laplacian of electron density $\nabla^2 p(r)$ lie in the range 0.013–0.016 e Å^{-5}. The values of total energy have three zeros after the point and have significant figures only at 4 decimal places; thus, these values can be considered as approximately zero. The third type of contact between cluster anions is the BH. . .HB one. The distances of BH. . .HB contacts are equal to 2.81 Å. The values of electron density $p(r)$ at bcp related to BH. . .HB contacts are equal to 0.003 e Å^{-3}. The values of Laplacian of electron density $\nabla^2 p(r)$ are equal to 0.010 e Å^{-5}. The values of total energy are approximately zero as in the case of CH. . .HB contacts.

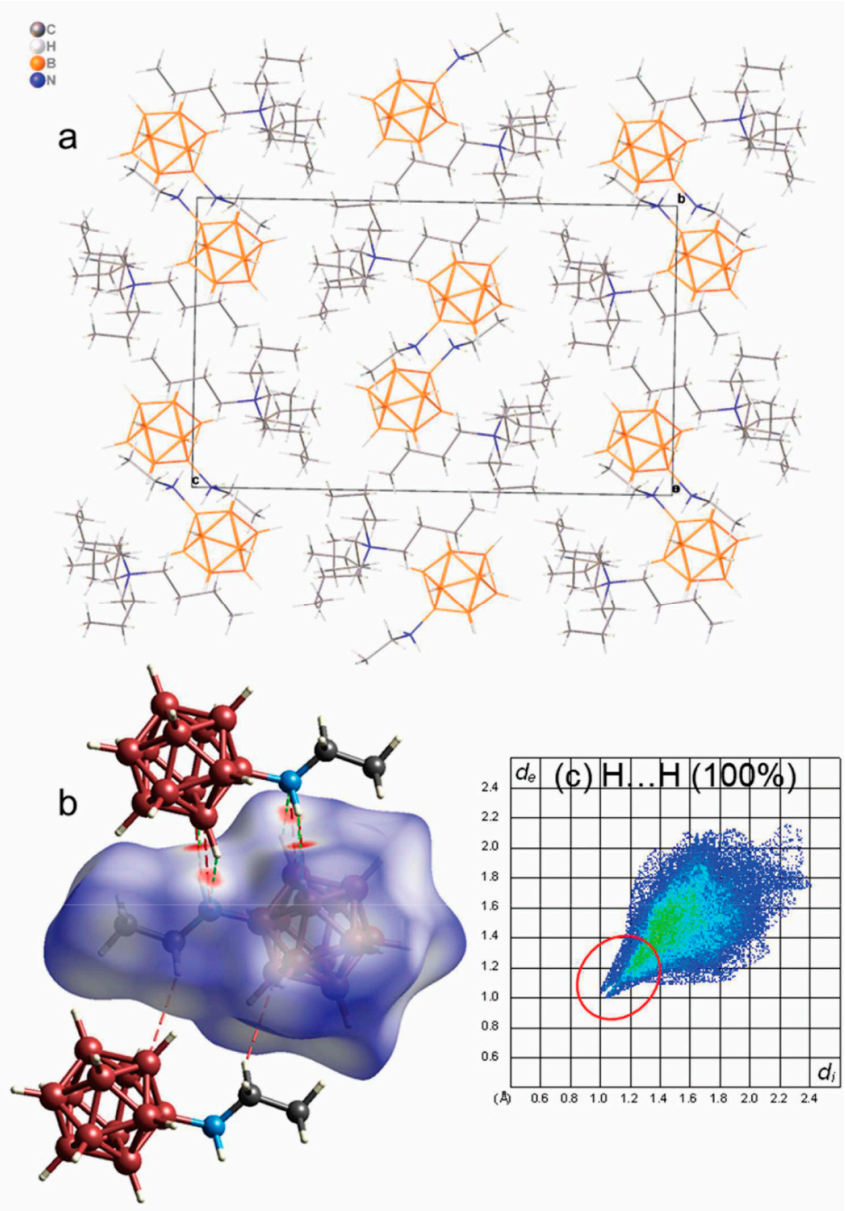


Figure 2. (**a**) Packing diagram, (**b**) d_{norm} surface of $[B_{12}H_{11}NH_2Et]^-$ anion for compound **2a**, (**c**) full two-dimensional fingerprint plot for **2a**. The area of NH. . .HB contacts, that are less than the sum of the van der Waals radii of hydrogen atoms, is highlighted with a red oval.

NH. . .HB contacts have large descriptor values compared to CH. . .HB and BH. . .HB contacts. Given contacts have the greatest values of electron density $p(r)$ and total energy H_b at bcp, whereas BH. . .HB contacts have the lowest values of these descriptors. Thus, one can conclude that the NH. . .HB contacts are the stronger ones, and BH. . .HB contacts are the weakest ones based on joint QTAIM and Hirshfeld analysis.

3. Materials and Methods

3.1. IR Spectra

IR spectra of the compounds were recorded on an IR Fourier-transform spectrophotometer Infralum FT-08 ("Lumex", St. Petersburg, Russia) in the range of 4000–400 cm^{-1} with a resolution of 1 cm^{-1}. Samples were prepared in the form of solutions in chloroform.

3.2. ^{1}H NMR, ^{11}B NMR, and ^{13}C NMR

^{1}H NMR, ^{11}B NMR, and ^{13}C NMR spectra of solutions of the investigated substances in CD_3CN were recorded on a pulse Fourier-transform spectrometer Bruker AVANCE-300 (Germany) at frequencies of 300.3, 96.32, and 75.49 MHz, respectively, with internal deuterium stabilization. Tetramethylsilane or boron trifluoride etherate was used as the external standard.

3.3. Electrospray Ionization Mass Spectrometry (ESI-MS)

An LC system consisting of two LC-20AD pumps (Shimadzu, Kyoto, Japan) and autosampler was coupled online with an LCMS-IT-TOF mass spectrometer equipped with an electrospray ionization source (Shimadzu, Japan). The HRMS spectra were acquired in direct injection mode without a column. Mass spectra were obtained in the *m/z* range from 120 to 700 Da (for negative ionization mode) and 100–700 for positive mode. Other MS parameters were as follows: detector voltage: 1.55 kV, nebulizing gas: 1.50 L/min, CDL temperature: 200.0 °C CDL, heat block temperature: 200.0 °C, ESI voltage: 4.50 kV, event time: 300 ms, repeats: 3, ion accumulation: 30 ms. Instrument tuning (mass calibration and sensitivity check) was carried out before analysis.

3.4. Preparative HPLC

Preparative HPLC was carried out on an isocratic HPLC system "STAYER" ("Akvilon", Moscow, Russia), with a spectrophotometric detector (UVV 104, with variable wavelength from 200 to 360 nm) using a Knauer Eurospher 110 Si column.

3.5. Single-Crystal X-ray Diffraction

Single-crystal X-ray diffraction data for **1** were collected on a three-circle Bruker D8 Venture diffractometer (T = 100 K, graphite monochromator, ω and ϕ scanning mode). The data were indexed and integrated using the SAINT (V7.60A) program [78] and then scaled and corrected for absorption using the SADABS (version 2008/1) program [79]. For details, see Table S1.

The structures were determined using direct methods and refined with the full-matrix least squares technique on F^2 with anisotropic displacement parameters for non-hydrogen atoms. The hydrogen atoms were placed in calculated positions and refined within the riding model with fixed isotropic displacement parameters (U_{iso}(H) = 1.5U_{eq}(O), 1.5U_{eq}(C) for the CH_3-groups and 1.2U_{eq}(C) for the other groups). All calculations were carried out using the SHELXTL program (version 2018/2) [80] and OLEX2 program (version 1.5) package [81].

The B-type alerts in crystal **2a** are due to poor crystal quality.

Crystallographic data for all investigated compounds have been deposited with the Cambridge Crystallographic Data Center, CCDC 2305164. Copies of this information may be obtained free of charge from the Director, CCDC, 12 Union Road, Cambridge CB2 1EZ, UK (Fax: +44-1223-336033, e-mail: deposit@ccdc.cam.ac.uk, or www.ccdc.cam.ac.uk (accessed on 15 December 2023).

3.6. Computational Details

For estimation of non-covalent contacts in the crystal structure of $(Bu_4N)[B_{12}H_{11}NH_2Et]$, the part of crystal unit including three boron clusters was chosen. The ORCA 4.2.1 software package was applied to perform calculation. A single-point computation for the model structure was performed at the ωB97X-D3/def2-TZVPP theory level using the atom-pairwise dispersion correction with the zero-damping scheme [82–84]. All calculations

were performed using the RIJCOSX approximation with the def2/J auxiliary basis set [85]. Tight criteria of SCF convergence ("Tight SCF") were employed for the calculations. The keywords "Grid5", "FinalGrid6", and "GridX5" were used as parameters for the spatial integration grid. For the model structures with closed electron shells, spin-restricted approximation was utilized. Topological analysis of the electron density distribution, based on the Quantum Theory of Atoms in Molecules (QTAIM) formalism developed by Bader [86,87], was employed with the Multiwfn program (version 3.7) [88].

3.7. Synthesis of Compounds

The reagent grade solvents were used without additional purification. Commercially available reagent grade lithium aluminum hydride (LAH) (95%) was purchased from Sigma Aldrich.

Synthesis of nitrile derivatives of *closo*-dodecaborate anion $(Bu_4N)[B_{12}H_{11}NCR]$:

The nitrilium derivatives (1 a–e) were obtained using a known methodology [58,62].

Synthesis of N-alkylammonium derivatives of the *closo*-dodecaborate anion. $(Bu_4N)_2[B_{12}H_{11}NH_2CH_2R]$

$(Bu_4N)[B_{12}H_{11}(NH_2CH_2CH_3)]$ 2a

General procedure

First, 0.38 g (10 mmol) of $LiAlH_4$ and 2 mL of tetrahydrofuran (THF) were placed into a flask. Then, 0.424 g (1 mmol) of **$(Bu_4N)[B_{12}H_{11}NCCH_3]$** was dissolved in 5 mL of THF. The solution of the nitrile derivative was slowly added to the $LiAlH_4$ suspension, and the mixture was stirred at room temperature for 2 h. To the reaction mixture, 10 mL of 1 N HCl was added dropwise until gas evolution ceased. The precipitated solid was filtered off and washed with 20 mL of acetonitrile. The filtrate was concentrated using a rotary evaporator, and 20 mL of diethyl ether was added to it. The mixture was then treated with ultrasound. The resulting precipitate was filtered, washed with diethyl ether, and dried under vacuum. Yield: 90%. $^{11}B\{H\}$ NMR (CD_3CN, ppm.): −4.6 (s, 1B, B-N), −15.8 (s, 10B, B-H(B2-11)), −17.9 (s, 1B, B-H (B12)). ^{1}H NMR (CD_3CN, ppm.): 2.5–0.0 (m, 11H, B-H), 3.08 (8H, Bu_4N), 1.6 (8H, Bu_4N), 1.35 (8H, Bu_4N), 0.96 (12H, Bu_4N), 4.86 (s, 2H, NH_2), 2.91 (m, 2H, $C\underline{H}_2CH_3$), 1.16 (t, 3H, $CH_2C\underline{H}_3$ J = 7.26 Hz). $^{13}C\{H\}$ NMR (CD_3CN, ppm.): 59.4 (Bu_4N), 24.4 (Bu_4N), 20.,2 (Bu_4N), 13.9 (Bu_4N), 44.0 ($\underline{C}H_2CH_3$), 14.1($CH_2\underline{C}H_3$). IR(CH_2Cl_2,cm^{-1}): 3224, 3205 ν (N-H), 2491 ν (B-H). MS(ESI) *m/z*: 186.2650 (A refers to the molecular weight of $[B_{12}H_{11}(NH_2CH_2CH_3)]$, calculated for {[A]-} 186.2629).

$(Bu_4N)[B_{12}H_{11}(NH_2{}^nC_3H_7)]$ 2b

Yield: 89%. $^{11}B\{H\}$ NMR (CD_3CN, ppm.): −4.6 (s, 1B, B-N), −15.9 (s, 10B, B-H(B2-11)), −17.9 (s, 1B, B-H (B12)). ^{1}H NMR (CD_3CN, ppm.): 2.5–0.0 (m, 11H, B-H), 3.15 (8H, Bu_4N), 1.61 (8H, Bu_4N), 1.45 (8H, Bu_4N), 1.01 (12H, Bu_4N), 4.87 (s, 2H, NH_2), 2.83 (m, 2H, $C\underline{H}_2CH_2CH_3$), 1.58 (m, 2H, $CH_2C\underline{H}_2CH_3$), 0.88 (t, 3H, $CH_2CH_2C\underline{H}_3$ J = 7.46 Hz). $^{13}C\{H\}$ NMR (CD_3CN, ppm.): 59.4 (Bu_4N), 24.4 (Bu_4N), 20.2 (Bu_4N), 13.9 (Bu_4N), 50.6 ($\underline{C}H_2CH_2CH_3$), 22.2 ($CH_2\underline{C}H_2CH_3$), 11.3 ($CH_2CH_2\underline{C}H_3$). IR(CH_2Cl_2, cm^{-1}): 3229, 3206 ν (N-H), 2491 ν (B-H). MS(ESI) *m/z*: 200,2810 (A refers to the molecular weight of $[B_{12}H_{11}(NH_2CH_2CH_2CH_3)]$, calculated for {[A]-} 200,2785).

$(Bu_4N)[B_{12}H_{11}(NH_2{}^nC_4H_9)]$ 2c

Yield: 86%. $^{11}B\{H\}$ NMR (CD_3CN, ppm.): −4.5 (c, 1B, B-N), −15.8 (s, 10B, B-H(B2-11)), −17.9 (s, 1B, B-H (B12)). ^{1}H NMR (CD_3CN, ppm.): 2.5–0.0 (m, 11H, B-H), 3.15 (8H, Bu_4N), 1.61 (8H, Bu_4N), 1.45 (8H, Bu_4N), 1.01 (12H, Bu_4N), 4.85 (s, 2H, NH_2), 2.85 (m, 2H, $C\underline{H}_2CH_2CH_2CH_3$), 1.59 (m, 2H, $CH_2C\underline{H}_2CH_2CH_3$), 1.33 (m, 2H, $CH_2CH_2C\underline{H}_2CH_3$), 0.89 (t, 3H, $CH_2CH_2CH_2C\underline{H}_3$ J = 7.36 Hz). $^{13}C\{H\}$ NMR (CD_3CN, ppm.): 59.4 (Bu_4N), 24.4 (Bu_4N), 20.2 (Bu_4N), 13.9 (Bu_4N), 48.8 ($\underline{C}H_2CH_2CH_2CH_3$), 31.0 ($CH_2\underline{C}H_2CH_2CH_3$), 20.5 ($CH_2CH_2\underline{C}H_2CH_3$), 14.0($CH_2CH_2CH_2\underline{C}H_3$). IR($CH_2Cl_2$, cm^{-1}): 3277, 3206 ν (N-H), 2492 ν (B-H). MS(ESI) *m/z*: 214,2966 (A refers to the molecular weight of $[B_{12}H_{11}(NH_2CH_2CH_2CH_2CH_3)]$, calculated for {[A]-} 214,2942).

$(Bu_4N)[B_{12}H_{11}(NH_2{}^iC_4H_9)]$ 2d

Yield: 79%. $^{11}B\{H\}$ NMR (CD_3CN, ppm.): −4.4 (s, 1B, B-N), −15.8 (s, 10B, B-H(B2-11)), −17.9 (s, 1B, B-H (B12)). ^1H NMR (CD_3CN, ppm.): 2.5–0.0 (m, 11H, B-H), 3.15 (8H, Bu_4N), 1.61 (8H, Bu_4N), 1.45 (8H, Bu_4N), 1.01 (12H, Bu_4N), 4.76 (s, 2H, NH_2), 2.73 (m, 2H, $C\underline{H}_2CH(CH_3)_2$), 1.88 (m, 1H, $CH_2C\underline{H}(CH_3)_2$), 0.9 (d, 6H, $CH_2CH(C\underline{H}_3)_2$ J = 6.7 Hz). $^{13}C\{H\}$ NMR (CD_3CN, ppm.): 59.4 (Bu_4N), 24.4 (Bu_4N), 20.2 (Bu_4N), 13.9 (Bu_4N), 56.3 ($C\underline{H}_2CH(CH_3)_2$), 27.7 ($CH_2\underline{C}H(CH_3)_2$), 20.3, 20.1 ($CH_2CH(\underline{C}H_3)_2$). IR ($CH_2Cl_2$, cm^{-1}): 3293, 3201 ν (N-H), 2493 ν (B-H). MS(ESI) *m/z*: 214,2968 (A refers to the molecular weight of $[B_{12}H_{11}(NH_2CH_2CH(CH_3)_2]$, calculated for {[A]-} 214,2942).

$(Bu_4N)[B_{12}H_{11}(NH_2C_6H_4CH_3)]$ 2e

This compound was obtained using a similar methodology.

Yield: 90%. $^{11}B\{H\}$ NMR (CD_3CN, ppm.): −4.3 (s, 1B, B-N), −15.8 (s, 10B, B-H(B2-11)), 17.8 (s, 1B, B-H(B12)). ^1H NMR (CD_3CN, ppm.): 2.5–0.0 (m, 11H, B-H), 7.25, (d, 2H, $C_6\underline{H}_4$ J = 7.91 Hz), 7.17 (d, 2H, $C_6\underline{H}_4$ J = 7.83 Hz), 5.23 (s, 2H, NH_2), 4.01 (M, 2H, $NH_2C\underline{H}_2C_6H_4CH_3$), 3.08 (8H, NBu_4), 2.32 (s, 3H, $NH_2CH_2C_6H_4C\underline{H}_3$), 1.60 (8H, NBu_4), 1.35 (8H, NBu_4), 0.97 (12H, NBu_4). ^{13}C NMR (CD_3CN, ppm): 139.2, 133.2, 130.1 ($NH_2CH_2\underline{C}_6H_4CH_3$), 59.4 ($NBu_4$), 52.7 ($NH_2\underline{C}H_2C_6H_4CH_3$), 24.3 ($NBu_4$), 21.1 ($NH_2CH_2C_6H_4\underline{C}H_3$), 20.3 ($NBu_4$), 13.8 ($NBu_4$). IR ($CH_2Cl_2$, cm^{-1}): 3288, 3197, 3122 ν (N-H), 2491 ν (B-H), 1635 ν (C=C). MS (ESI) *m/z*: 262.2964 (A refers to the molecular weight of $[B_{12}H_{11}(NH_2CH_2C_6H_4CH_3)]$, calculated for {[A]-} 262.2942).

4. Conclusions

During this work, a technique for selectively obtaining N-alkylammonium derivatives of the *closo*-dodecaborate anion $[B_{12}H_{11}NH_2CH_2R]^-$ by reducing the corresponding nitrile derivatives $[B_{12}H_{11}NCR]^-$ with lithium aluminum hydride ($LiAlH_4$) was developed. A series of N-alkylammonium derivatives with different substituents R were obtained, including Me (methyl), Et (ethyl), nPr (n-propyl), nPr (isopropyl), and p-tolyl. The analysis of the crystal structure $(Bu_4N)[B_{12}H_{11}(NH_2CH_2CH_3)]$ showed that anions form dimeric pairs linked by NH. . .HB dihydrogen bonds.

Supplementary Materials: The following supporting information can be downloaded at: https://www.mdpi.com/article/10.3390/inorganics12010002/s1, Figure S1: 11B{1H} NMR spectrum $(Bu_4N)[B_{12}H_{11}NH_2CH_2CH_3]$ 2a; Figure S2: ^1H NMR spectrum $(Bu_4N)[B_{12}H_{11}NH_2CH_2CH_3]$ 2a; Figure S3: 13C NMR spectrum $(Bu_4NN)[B_{12}H_{11}NH_2CH_2CH_3]$ 2a; Figure S4: ESI-MS spectrum $(Bu_4N)[B_{12}H_{11}NH_2CH_2CH_3]$ 2a (negative area) 1; Figure S5: 11B{1H} NMR spectrum $(Bu_4N)[B_{12}H_{11}NH_2CH_2CH_2CH_3]$ 2b; Figure S6: 1H NMR spectrum $(Bu_4N)[B_{12}H_{11}NH_2CH_2CH_2CH_3]$ 2b; Figure S7: 13C NMR spectrum $(Bu_4N)[B_{12}H_{11}NH_2CH_2CH_2CH_3]$ 2b; Figure S8: ESI-MS spectrum $(Bu_4N)[B_{12}H_{11}NH_2CH_2CH_2CH_3]$ 2b (negative area).; Figure S9: $^{11}B\{^1H\}$ NMR spectrum $(Bu_4N)[B_{12}H_{11}NH_2CH_2CH_2CH_2CH_3]$ 2c; Figure S10: ^1H NMR spectrum $(Bu_4N)[B_{12}H_{11}NH_2CH_2CH_2CH_2CH_3]$ 2c; Figure S11: ^{13}C NMR spectrum $(Bu_4N)[B_{12}H_{11}NH_2CH_2CH_2CH_2CH_3]$ 2c; Figure S12: ESI-MS spectrum $(Bu_4N)[B_{12}H_{11}NH_2CH_2CH_2CH_2CH_3]$ 2c (negative area).; Figure S13: $^{11}B\{^1H\}$ NMR spectrum $(Bu_4N)[B_{12}H_{11}NH_2CH_2CH(CH_3)_2]$ 2d; Figure S14: ^1H NMR spectrum $(Bu_4N)[B_{12}H_{11}NH_2CH_2CH(CH_3)_2]$ 2d; Figure S15: 13C NMR spectrum $(Bu_4N)[B_{12}H_{11}NH_2CH_2CH(CH_3)_2]$ 2d; Figure S16: ESI-MS spectrum $(Bu_4N)[B_{12}H_{11}NH_2CH_2CH(CH_3)_2]$ 2d (negative area).; Figure S17: $^{11}B\{^1H\}$ NMR spectrum $(Bu_4N)[B_{12}H_{11}NH_2CH_2C_6H_4CH_3]$ 2e; Figure S18: ^1H NMR spectrum $(Bu_4N)[B_{12}H_{11}NH_2CH_2C_6H_4CH_3]$ 2e; Figure S19: ^{13}C NMR spectrum $(Bu_4N)[B_{12}H_{11}NH_2CH_2C_6H_4CH_3]$ 2e; Figure S20: ESI-MS spectrum $(Bu_4N)[B_{12}H_{11}NH_2CH_2C_6H_4CH_3]$ 2e (negative area).; Figure S21: Molecular graph showing the results of the topological analysis of the electron density distribution in the model structure of the trimer of $[B_{12}H_{11}NH_2CH_2CH_3]^-$.

Author Contributions: Manuscript conception, A.P.Z. and K.Y.Z.; writing and original draft preparation, A.V.N., N.K.N. and A.P.Z.; synthesis of derivatives, A.V.N. and N.K.N.; NMR analysis, N.A.S. and A.Y.B.; X-ray analysis and Hirshfeld surface analysis, A.S.K.; editing, data analysis, and interpretation, I.N.K., A.S.N., A.P.Z. and K.Y.Z.; supervision, K.Y.Z. and N.T.K. All authors have read and agreed to the published version of the manuscript.

Funding: The work was supported by the Ministry of Science and Higher Education of the Russian Federation. Agreement No. 075-15-2020-782.

Institutional Review Board Statement: Not applicable.

Informed Consent Statement: Not applicable.

Data Availability Statement: Data are contained within the article and Supplementary Materials.

Acknowledgments: A.S.N. is grateful to the RUDN University Strategic Academic Leadership Program.

Conflicts of Interest: The authors declare no conflict of interest.

References

1. Nakamura, H.; Kirihata, M. Boron Compounds: New Candidates for Boron Carriers in BNCT. In *Neutron Capture Therapy*; Springer: Berlin/Heidelberg, Germany, 2012; pp. 99–116.
2. Pitto-Barry, A. Polymers and Boron Neutron Capture Therapy (BNCT): A Potent Combination. *Polym. Chem.* **2021**, *12*, 2035–2044. [CrossRef]
3. Novopashina, D.S.; Vorobyeva, M.A.; Venyaminova, A. Recent Advances in the Synthesis of High Boron-Loaded Nucleic Acids for BNCT. *Front. Chem.* **2021**, *9*, 619052. [CrossRef]
4. Tjarks, W. The Use of Boron Clusters in the Rational Design of Boronated Nucleosides for Neutron Capture Therapy of Cancer. *J. Organomet. Chem.* **2000**, *614–615*, 37–47. [CrossRef]
5. Leśnikowski, Z.J. What Are the Current Challenges with the Application of Boron Clusters to Drug Design? *Expert. Opin. Drug Discov.* **2021**, *16*, 481–483. [CrossRef]
6. Gentil, S.; Crespo, E.; Rojo, I.; Friang, A.; Viñas, C.; Teixidor, F.; Grüner, B.; Gabel, D. Polypyrrole Materials Doped with Weakly Coordinating Anions: Influence of Substituents and the Fate of the Doping Anion during the Overoxidation Process. *Polymer* **2005**, *46*, 12218–12225. [CrossRef]
7. Axtell, J.C.; Saleh, L.M.A.; Qian, E.A.; Wixtrom, A.I.; Spokoyny, A.M. Synthesis and Applications of Perfunctionalized Boron Clusters. *Inorg. Chem.* **2018**, *57*, 2333–2350. [CrossRef]
8. Jenne, C.; Wegener, B. Silver Salts of the Weakly Coordinating Anion $[Me_3NB_{12}Cl_{11}]^-$. *Z. Anorg. Allg. Chem.* **2018**, *644*, 1123–1132. [CrossRef]
9. Nieuwenhuyzen, M.; Seddon, K.R.; Teixidor, F.; Puga, A.V.; Viñas, C. Ionic Liquids Containing Boron Cluster Anions. *Inorg. Chem.* **2009**, *48*, 889–901. [CrossRef]
10. Spokoyny, A.M. New Ligand Platforms Featuring Boron-Rich Clusters as Organomimetic Substituents. *Pure Appl. Chem.* **2013**, *85*, 903–919. [CrossRef]
11. Grimes, R.N. Boron-Carbon Ring Ligands in Organometallic Synthesis. *Chem. Rev.* **1992**, *92*, 251–268. [CrossRef]
12. Kirlikovali, K.O.; Axtell, J.C.; Gonzalez, A.; Phung, A.C.; Khan, S.I.; Spokoyny, A.M. Luminescent Metal Complexes Featuring Photophysically Innocent Boron Cluster Ligands. *Chem. Sci.* **2016**, *7*, 5132–5138. [CrossRef]
13. Bolze, F.; Hayek, A.; Sun, X.H.; Baldeck, P.L.; Bourgogne, C.; Nicoud, J.F. New Insight in Boron Chemistry: Application in Two-Photon Absorption. *Opt. Mater.* **2011**, *33*, 1453–1458. [CrossRef]
14. Omidvar, A. Nonlinear Optical Response of Teetotum Boron Clusters. *Comput. Theor. Chem.* **2021**, *1198*, 113178. [CrossRef]
15. Lin, Z.; Yang, G. Oxo Boron Clusters and Their Open Frameworks. *Eur. J. Inorg. Chem.* **2011**, *2011*, 3857–3867. [CrossRef]
16. Mukherjee, S.; Thilagar, P. Boron Clusters in Luminescent Materials. *Chem. Commun.* **2016**, *52*, 1070–1093. [CrossRef]
17. Allis, D.G.; Spencer, J.T. Polyhedral-Based Nonlinear Optical Materials. 2.[1] Theoretical Investigation of Some New High Nonlinear Optical Response Compounds Involving Polyhedral Bridges with Charged Aromatic Donors and Acceptors. *Inorg. Chem.* **2001**, *40*, 3373–3380. [CrossRef]
18. Scheifers, J.P.; Zhang, Y.; Fokwa, B.P.T. Boron: Enabling Exciting Metal-Rich Structures and Magnetic Properties. *Acc. Chem. Res.* **2017**, *50*, 2317–2325. [CrossRef]
19. Oleshkevich, E.; Teixidor, F.; Rosell, A.; Viñas, C. Merging Icosahedral Boron Clusters and Magnetic Nanoparticles: Aiming toward Multifunctional Nanohybrid Materials. *Inorg. Chem.* **2018**, *57*, 462–470. [CrossRef]
20. Dash, B.P.; Satapathy, R.; Maguire, J.A.; Hosmane, N.S. Polyhedral Boron Clusters in Materials Science. *New J. Chem.* **2011**, *35*, 1955. [CrossRef]
21. Mori, T. Thermoelectric and Magnetic Properties of Rare Earth Borides: Boron Cluster and Layered Compounds. *J. Solid. State Chem.* **2019**, *275*, 70–82. [CrossRef]
22. Qi, B.; Wu, C.; Li, X.; Wang, D.; Sun, L.; Chen, B.; Liu, W.; Zhang, H.; Zhou, X. Self-Assembled Magnetic Gold Catalysts from Dual-Functional Boron Clusters. *ChemCatChem* **2018**, *10*, 2285–2290. [CrossRef]
23. Wang, Z.; Wang, Z.; Ma, X.; Liu, Y.; Zhang, H. Direct Conversion of Methane into Methanol and Ethanol via Spherical Au@Cs_2[*Closo*-$B_{12}H_{12}$] and Pd@Cs_2[*Closo*-$B_{12}H_{12}$] Nanoparticles. *Int. J. Hydrogen Energy* **2021**, *46*, 30750–30761. [CrossRef]
24. Wang, L.; Sun, W.; Duttwyler, S.; Zhang, Y. Efficient Adsorption Separation of Methane from CO_2 and C2–C3 Hydrocarbons in a Microporous *Closo*-Dodecaborate $[B_{12}H_{12}]^{2-}$ Pillared Metal–Organic Framework. *J. Solid. State Chem.* **2021**, *299*, 122167. [CrossRef]

25. Wang, Z.; Liu, Y.; Zhang, H.; Zhou, X. Cubic Platinum Nanoparticles Capped with Cs_2[*Closo*-$B_{12}H_{12}$] as an Effective Oxidation Catalyst for Converting Methane to Ethanol. *J. Colloid. Interface Sci.* **2020**, *566*, 135–142. [CrossRef]
26. Raghuwanshi, M.; Lanterne, A.; le Perchec, J.; Pareige, P.; Cadel, E.; Gall, S.; Duguay, S. Influence of Boron Clustering on the Emitter Quality of Implanted Silicon Solar Cells: An Atom Probe Tomography Study. *Prog. Photovolt. Res. Appl.* **2015**, *23*, 1724–1733. [CrossRef]
27. Krishnan, S.; Senthilkumar, K. Opto-Electronic Properties of Quasi-Planar Boron Clusters—A DFT Investigation. *Chem. Phys. Lett.* **2022**, *804*, 139914. [CrossRef]
28. Ma, Z.Q.; Liu, B.X. Boron-Doped Diamond-like Amorphous Carbon as Photovoltaic Films in Solar Cell. *Sol. Energy Mater. Sol. Cells* **2001**, *69*, 339–344. [CrossRef]
29. Sivaev, I.B.; Bregadze, V.I.; Sjöberg, S. Chemistry of *Closo*-Dodecaborate Anion $[B_{12}H_{12}]^{2-}$: A Review. *Collect. Czechoslov. Chem. Commun.* **2002**, *67*, 679–727. [CrossRef]
30. Geis, V.; Guttsche, K.; Knapp, C.; Scherer, H.; Uzun, R. Synthesis and Characterization of Synthetically Useful Salts of the Weakly-Coordinating Dianion $[B_{12}Cl_{12}]^{2-}$. *Dalton Trans.* **2009**, *15*, 2684–2687. [CrossRef]
31. Peryshkov, D.V.; Popov, A.A.; Strauss, S.H. Direct Perfluorination of $K_2B_{12}H_{12}$ in Acetonitrile Occurs at the Gas Bubble−Solution Interface and Is Inhibited by HF. Experimental and DFT Study of Inhibition by Protic Acids and Soft, Polarizable Anions. *J. Am. Chem. Soc.* **2009**, *131*, 18393–18403. [CrossRef]
32. Pluntze, A.M.; Bukovsky, E.V.; Lacroix, M.R.; Newell, B.S.; Rithner, C.D.; Strauss, S.H. Deca-B-Fluorination of Diammonioboranes. Structures and NMR Characterization of 1,2-, 1,7-, and 1,12-$B_{12}H_{10}(NH_3)_2$ and 1,2-, 1,7-, and 1,12-$B_{12}F_{10}(NH_3)_2$. *J. Fluor. Chem.* **2018**, *209*, 33–42. [CrossRef]
33. Tiritiris, I.; Schleid, T. The Crystal Structure of Solvent-Free Silver Dodecachloro-*Closo*-dodecaborate $Ag_2[B_{12}Cl_{12}]$ from Aqueous Solution. *Z. Anorg. Allg. Chem.* **2003**, *629*, 581–583. [CrossRef]
34. Bayer, M.J.; Hawthorne, M.F. An Improved Method for the Synthesis of [*Closo*-$B_{12}(OH)_{12}]^{-2}$. *Inorg. Chem.* **2004**, *43*, 2018–2020. [CrossRef]
35. Bondarev, O.; Khan, A.A.; Tu, X.; Sevryugina, Y.V.; Jalisatgi, S.S.; Hawthorne, M.F. Synthesis of [*Closo*-$B_{12}(OH)_{11}NH_3]^-$: A New Heterobifunctional Dodecaborane Scaffold for Drug Delivery Applications. *J. Am. Chem. Soc.* **2013**, *135*, 13204–13211. [CrossRef]
36. Knoth, W.H.; Sauer, J.C.; Balthis, J.H.; Miller, H.C.; Muetterties, E.L. Boranes. XXX. Carbonyl derivatives of $B_{10}H_{10}^{2-}$ and $B_{12}H_{12}^{2-}$. *J. Am. Chem. Soc.* **1967**, *3973*, 4842–4850. [CrossRef]
37. Srebny, H.-G.; Preetz, W.; Marsmann, H.C. Darstellung, 11B-NMR- Und Schwingungsspektren Isomerenreiner Halogenhydrodecaborate $X_nB_{12}H_{12-n}^{2-}$; X = Cl, n = 1–3, X = Br, n =1,2; X = I, n =1. *Z. Naturforschung B* **1984**, *39*, 189–196. [CrossRef]
38. Knoth, W.H.; Sauer, J.C.; England, D.C.; Hertler, W.R.; Muetterties, E.L. Chemistry of Boranes. XIX. 1 Derivative Chemistry of $B_{10}H_{10}^{-2}$ and $B_{12}H_{12}^{-2}$. *J. Am. Chem. Soc.* **1964**, *86*, 3973–3983. [CrossRef]
39. Hertler, W.R.; Raasch, M.S. Chemistry of Boranes. XIV. Amination of $B_{10}H_{10}^{-2}$ and $B_{12}H_{12}^{-2}$ with Hydroxylamine-O-Sulfonic Acid. *J. Am. Chem. Soc.* **1964**, *86*, 3661–3668. [CrossRef]
40. Zhao, X.; Yang, Z.; Chen, H.; Wang, Z.; Zhou, X.; Zhang, H. Progress in Three-Dimensional Aromatic-like *Closo*-Dodecaborate. *Coord. Chem. Rev.* **2021**, *444*, 214042. [CrossRef]
41. Sivaev, I.B.; Semioshkin, A.A.; Brellochs, B.; Sjoberg, S.; Bregadze, V.I. Synthesis of Oxonium Derivatives of the Dodecahydro-closo-dodecaborate anion $[B_{12}H_{12}]^{2-}$. *Polyhedron.* **2000**, *19*, 627–632. [CrossRef]
42. Hattori, Y.; Kusaka, S.; Mukumoto, M.; Ishimura, M.; Ohta, Y.; Takenaka, H.; Uehara, K.; Asano, T.; Suzuki, M.; Masunaga, S.; et al. Synthesis and in vitro Evaluation of Thiododecaborated α, α-Cycloalkylamino Acids for the Treatment of Malignant Brain Tumors by Boron Neutron Capture Therapy. *Amino Acids* **2014**, *46*, 2715–2720. [CrossRef] [PubMed]
43. He, T.; Musah, R.A. Evaluation of the Potential of 2-Amino-3-(1,7-Dicarba- *Closo*-Dodecaboranyl-1-Thio)Propanoic Acid as a Boron Neutron Capture Therapy Agent. *ACS Omega* **2019**, *4*, 3820–3826. [CrossRef]
44. Nagasawa, K.; Narisada, M. Synthesis of Polyhedral Borane Derivatives Having a Carboxy Group. *Tetrahedron Lett.* **1990**, *31*, 4029–4032. [CrossRef]
45. Nagasawa, K.; Ikenishi, Y.; Nakagawa, Y. Oxidation Products of Cesium Monomercaptoundecahydro-*Closo*-Dodecaborate(2−). *J. Organomet. Chem.* **1990**, *391*, 139–146. [CrossRef]
46. Goswami, L.N.; Ma, L.; Cai, Q.; Sarma, S.J.; Jalisatgi, S.S.; Frederick Hawthorne, M. CRGD Peptide-Conjugated Icosahedral *Closo*-B_{12}^{2-} Core Carrying Multiple Gd^{3+}-DOTA Chelates for Avβ3 Integrin-Targeted Tumor Imaging (MRI). *Inorg. Chem.* **2013**, *52*, 1701–1709. [CrossRef] [PubMed]
47. Goswami, L.N.; Chakravarty, S.; Cai, Q.-Y.; Shapiro, E.M.; Frederick Hawthorne, M.; Ma, L. Amphiphilic DTPA Multimer Assembled on Icosahedral *Closo*-Borane Motif as High-Performance MRI Blood Pool Contrast Agent. *ACS Appl. Bio Mater.* **2021**, *4*, 6658–6663. [CrossRef] [PubMed]
48. Semioshkin, A.A.; Sivaev, I.B.; Bregadze, V.I. Cyclic Oxonium Derivatives of Polyhedral Boron Hydrides and Their Synthetic Applications. *Dalton Trans.* **2008**, *11*, 977–992. [CrossRef]
49. Prikaznov, A.V.; Shmal'ko, A.V.; Sivaev, I.B.; Petrovskii, P.V.; Bragin, V.I.; Kisin, A.V.; Bregadze, V.V. Synthesis of Carboxylic Acids Based on the *Closo*-Decaborate Anion. *Polyhedron* **2011**, *30*, 1494–1501. [CrossRef]
50. Himmelspach, A.; Finze, M.; Vöge, A.; Gabel, D. Cesium and Tetrabutylammonium Salt of the Ethynyl-*Closo*-Dodecaborate Dianion. *Z. Anorg. Allg. Chem.* **2012**, *638*, 512–519. [CrossRef]

51. Peymann, T.; Knobler, C.B.; Hawthorne, M.F. Synthesis of Alkyl and Aryl Derivatives of *Closo*-$B_{12}H_{12}^{2-}$ by the Palladium-Catalyzed Coupling of *Closo*-$B_{12}H_{11}I^{2-}$ with Grignard Reagents. *Inorg. Chem.* **1998**, *37*, 1544–1548. [CrossRef]
52. Kaszyński, P.; Ringstrand, B. Functionalization of *Closo*-Borates via Iodonium Zwitterions. *Angew. Chem.-Int. Ed.* **2015**, *54*, 6576–6581. [CrossRef] [PubMed]
53. Tokarz, P.; Kaszyński, P.; Domagała, S.; Woźniak, K. The [*Closo*-$B_{12}H_{11}$-1-IAr]− Zwitterion as a Precursor to Monosubstituted Derivatives of [*Closo*-$B_{12}H_{12}]^{2-}$. *J. Organomet. Chem.* **2015**, *798*, 70–79. [CrossRef]
54. Sivaev, I.B.; Bruskin, A.B.; Nesterov, V.V.; Antipin, M.Y.; Bregadze, V.I.; Sjöberg, S. Synthesis of Schiff Bases Derived from the Ammoniaundecahydro-*Closo*-Dodecaborate(1−) Anion, $[B_{12}H_{11}NHCHR]^-$, and Their Reduction into Monosubstituted Amines $[B_{12}H_{11}NH_2CH_2R]^-$: A New Route to Water Soluble Agents for BNCT. *Inorg. Chem.* **1999**, *38*, 5887–5893. [CrossRef]
55. Justus, E.; Vöge, A.; Gabel, D. *N*-Alkylation of Ammonioundecahydro-*Closo*-dodecaborate(1–) for the Preparation of Anions for Ionic Liquids. *Eur. J. Inorg. Chem.* **2008**, *2008*, 5245–5250. [CrossRef]
56. Peymann, T.; Lork, E.; Schmidt, M.; Nöth, H.; Gabel, D. N-Alkylation of Ammine—Undecahydro-*Closo*-Dodecaborate(1−). *Chem. Ber.* **1997**, *130*, 795–799. [CrossRef]
57. Nelyubin, A.V.; Selivanov, N.A.; Bykov, A.Y.; Klyukin, I.N.; Novikov, A.S.; Zhdanov, A.P.; Karpechenko, N.Y.; Grigoriev, M.S.; Zhizhin, K.Y.; Kuznetsov, N.T. Primary Amine Nucleophilic Addition to Nitrilium *Closo*-Dodecaborate $[B_{12}H_{11}NCCH_3]$−: A Simple and Effective Route to the New BNCT Drug Design. *Int. J. Mol. Sci.* **2021**, *22*, 13391. [CrossRef] [PubMed]
58. Stogniy, M.Y.; Erokhina, S.A.; Sivaev, I.B.; Bregadze, V.I. Nitrilium Derivatives of Polyhedral Boron Compounds (Boranes, Carboranes, Metallocarboranes): Synthesis and Reactivity. *Phosphorus Sulfur. Silicon Relat. Elem.* **2019**, *194*, 983–988. [CrossRef]
59. Laskova, J.; Ananiev, I.; Kosenko, I.; Serdyukov, A.; Stogniy, M.; Sivaev, I.; Grin, M.; Semioshkin, A.; Bregadze, V.I. Nucleophilic Addition Reactions to Nitrilium Derivatives $[B_{12}H_{11}NCCH_3]^-$ and $[B_{12}H_{11}NCCH_2CH_3]^-$. Synthesis and Structures of *Closo*-Dodecaborate-Based Iminols, Amides and Amidines. *Dalton Trans.* **2022**, *51*, 3051–3059. [CrossRef]
60. Nelyubin, A.V.; Klyukin, I.N.; Novikov, A.S.; Zhdanov, A.P.; Selivanov, N.A.; Bykov, A.Y.; Kubasov, A.S.; Zhizhin, K.Y.; Kuznetsov, N.T. New Aspects of the Synthesis of *Closo*-Dodecaborate Nitrilium Derivatives $[B_{12}H_{11}NCR]^-$ (R = n-C_3H_7, i-C_3H_7, 4-$C_6H_4CH_3$, 1-$C_{10}H_7$): Experimental and Theoretical Studies. *Inorganics* **2022**, *10*, 196. [CrossRef]
61. Zhdanov, A.P.; Voinova, V.V.; Klyukin, I.N.; Kubasov, A.S.; Zhizhin, K.Y.; Kuznetsov, N.T. New Synthesis Method of N-Monosubstituted Ammonium-*Closo*-Decaborates. *J. Clust. Sci.* **2019**, *30*, 1327–1333. [CrossRef]
62. Ashby, E.C.; Dobbs, F.R.; Hopkins, H.P. Composition of Lithium Aluminum Hydride, Lithium Borohydride, and Their Alkoxy Derivatives in Ether Solvents as Determined by Molecular Association and Conductance Studies. *J. Am. Chem. Soc.* **1975**, *97*, 3158–3162. [CrossRef]
63. Guo, Z.; Sindelar, R.D. A New Preparation of Esters from Carbonyl Compounds Following Lithium Aluminum Hydride Reduction. *Synth. Commun.* **1998**, *28*, 1031–1039. [CrossRef]
64. Brown, H.C.; Weissman, P.M.; Yoon, N.M. Selective Reductions. IX. Reaction of Lithium Aluminum Hydride with Selected Organic Compounds Containing Representative Functional Groups[1]. *J. Am. Chem. Soc.* **1966**, *88*, 1458–1463. [CrossRef]
65. Newman, M.S.; Fukunaga, T. The Reduction of Amides to Amines via Nitriles by Lithium Aluminum Hydride[1]. *J. Am. Chem. Soc.* **1960**, *82*, 693–696. [CrossRef]
66. Sruthi, P.R.; Anas, S. An Overview of Synthetic Modification of Nitrile Group in Polymers and Applications. *J. Polym. Sci.* **2020**, *58*, 1039–1061. [CrossRef]
67. Moshnenko, N.; Kazantsev, A.; Chupakhin, E.; Bakulina, O.; Dar'in, D. Synthetic Routes to Approved Drugs Containing a Spirocycle. *Molecules* **2023**, *28*, 4209. [CrossRef]
68. Di Gioia, M.L.; Belsito, E.L.; Leggio, A.; Leotta, V.; Romio, E.; Siciliano, C.; Liguori, A. Reduction of Amide Carbonyl Group and Formation of Modified Amino Acids and Dipeptides. *Tetrahedron Lett.* **2015**, *56*, 2062–2066. [CrossRef]
69. Ambrosi, A.; Chua, C.K.; Bonanni, A.; Pumera, M. Lithium Aluminum Hydride as Reducing Agent for Chemically Reduced Graphene Oxides. *Chem. Mater.* **2012**, *24*, 2292–2298. [CrossRef]
70. Amundsen, L.H.; Nelson, L.S. Reduction of Nitriles to Primary Amines with Lithium Aluminum Hydride[1]. *J. Am. Chem. Soc.* **1951**, *73*, 242–244. [CrossRef]
71. Glaser, R.; Ulmer, L.; Coyle, S. Mechanistic Models for LAH Reductions of Acetonitrile and Malononitrile. Aggregation Effects of Li^+ and AlH_3 on Imide–Enamide Equilibria. *J. Org. Chem.* **2013**, *78*, 1113–1126. [CrossRef]
72. Málek, J. Reductions by Metal Alkoxyaluminum Hydrides. In *Organic Reactions*; Wiley: Hoboken, NJ, USA, 1985; pp. 1–317.
73. Li, H.; Zhang, Y.; Liu, L.; Jiao, N.; Meng, X.; Zhang, S. Amino Functionalized $[B_{12}H_{12}]^{2-}$ Salts as Hypergolic Fuels. *New J. Chem.* **2018**, *42*, 3568–3573. [CrossRef]
74. Gainsford, G.J.; Bowden, M.E. Propylamine–Borane. *Acta Crystallogr. Sect. E Struct. Rep. Online* **2009**, *65*, o1395. [CrossRef] [PubMed]
75. Ting, H.-Y.; Watson, W.H.; Kelly, H.C. Molecular and Crystal Structure of Ethylenediamine-Bisborane, $C_2H_{14}B_2N_3$. *Inorg. Chem.* **1972**, *11*, 374–377. [CrossRef]
76. Nelyubin, A.V.; Klyukin, I.N.; Novikov, A.S.; Zhdanov, A.P.; Grigoriev, M.S.; Zhizhin, K.Y.; Kuznetsov, N.T. Nucleophilic Addition of Amino Acid Esters to Nitrilium Derivatives of *Closo*-Decaborate Anion. *Mendeleev Commun.* **2021**, *31*, 201–203. [CrossRef]
77. Rattle, H.W.E. NMR of Amino Acids, Peptides, and Proteins (1977–1979). In *Annual Reports on NMR Spectroscopy*; Academic Press: Cambridge, MA, USA, 1981; Volume 11, pp. 1–64.
78. Bruker. *SAINT*; Bruker AXS Inc.: Madison, WI, USA, 2019.

79. Krause, L.; Herbst-Irmer, R.; Sheldrick, G.M.; Stalke, D. Comparison of Silver and Molybdenum Microfocus X-ray Sources for Single-Crystal Structure Determination. *J. Appl. Crystallogr.* **2015**, *48*, 3–10. [CrossRef]
80. Sheldrick, G.M. Crystal Structure Refinement with SHELXL. *Acta Crystallogr. C Struct. Chem.* **2015**, *71*, 3–8. [CrossRef]
81. Dolomanov, O.V.; Bourhis, L.J.; Gildea, R.J.; Howard, J.A.K.; Puschmann, H. OLEX2: A Complete Structure Solution, Refinement and Analysis Program. *J. Appl. Crystallogr.* **2009**, *42*, 339–341. [CrossRef]
82. Neese, F. The ORCA Program System. *WIREs Comput. Mol. Sci.* **2012**, *2*, 73–78. [CrossRef]
83. Grimme, S.; Antony, J.; Ehrlich, S.; Krieg, H. A Consistent and Accurate Ab Initio Parametrization of Density Functional Dispersion Correction (DFT-D) for the 94 Elements H-Pu. *J. Chem. Phys.* **2010**, *132*, 154104. [CrossRef]
84. Weigend, F.; Ahlrichs, R. Balanced Basis Sets of Split Valence, Triple Zeta Valence and Quadruple Zeta Valence Quality for H to Rn: Design and Assessment of AccuracyElectronic Supplementary Information (ESI) Available: [DETAILS]. *Phys. Chem. Chem. Phys.* **2005**, *7*, 3297–3305. [CrossRef]
85. Weigend, F. Accurate Coulomb-Fitting Basis Sets for H to Rn. *Phys. Chem. Chem. Phys.* **2006**, *8*, 1057–1065. [CrossRef] [PubMed]
86. Bader, R.F.W. *Atoms in Molecules: A Quantum Theory*; Oxford University Press: Oxford, UK, 1990.
87. Bader, R.; Legare, D. Properties of Atoms in Molecules: Structures and Reactivities of Boranes and Carboranes. *Can. J. Chem.* **1992**, *70*, 657–677. [CrossRef]
88. Lu, T.; Chen, F. Multiwfn: A Multifunctional Wavefunction Analyzer. *J. Comp. Chem.* **2011**, *33*, 580–592. [CrossRef] [PubMed]

Disclaimer/Publisher's Note: The statements, opinions and data contained in all publications are solely those of the individual author(s) and contributor(s) and not of MDPI and/or the editor(s). MDPI and/or the editor(s) disclaim responsibility for any injury to people or property resulting from any ideas, methods, instructions or products referred to in the content.